

# Commissioning of the Hanle Autoguider

Copenhagen University Observatory  
Edited November 10, 2005



**Figure 1:** First light image for the Hanle autoguider, obtained on September 17, 2005. A 5 second exposure of a field in Cygnus, not entirely in focus.

## Table of contents:

PSF variation.....	2
Focus pyramid.....	4
Throughput.....	4
Guiding performance.....	5
Vignetting .....	6
Pixel scale .....	6
References.....	7

This report describes the results of tests made at commissioning of the CUO-built autoguider at Hanle Observatory, during September 17-21, 2005.

## PSF variation

Full frame through-focus sequences in a field near the galaxy plane were obtained on two occasions. In addition of providing the value for best focus, analysis of these may reveal possible optics misalignment.

The first sequence was in mediocre seeing and with a high fraction of cloud cover: several exposures had to be repeated due to too dense clouds. Using HFOSC focus exposures, telescope focus was set to -1.135mm.

The autoguider camera focus was varied, resulting in the sequence in the table below.

AG-Focus	Mean FWHM (Pixels)	# stars	X-gradient	Y-gradient
1700	7.32	48	0.3	-0.4
1800	6.41	42	0.8	-0.9
1900	5.85	89	0.4	0.1
2000	5.22	67	0.2	0.0
2100	5.11	7	N/A	N/A
2200	4.26	114	-0.1	0.3
2300	4.70	70	0.2	1.1
2400	5.33	120	-0.6	1.2

A best focus is achieved for AG-focus=2200.

There is some tendency for a systematic skew of the FWHM field dependency. Part of this is due to the off-axis setup, but may also be due to misalignment, which will be examined below. The scale of the gradient is FWHM pixels over the full AG field.

A shorter sequence was made later, in better sky conditions. The telescope focus and focal plane tilt was adjusted by staff to a best value of -1.150mm for HFOSC. An AG camera focus of 2000 units was used, which was not the optimum value, as can be seen from both tables.

Tel-Focus (mm)	Mean FWHM (pixels)	# stars	X-gradient	Y-gradient
-1.130	5.77	111	0.3	-0.4
-1.150	4.26	182	-0.2	-0.3
-1.170	4.19	185	0.0	-0.2

The FWHM distribution is plotted in Figure 2 and Figure 3 for telescope focus of -1.170mm. The field variation can be seen to be approx.  $\pm 0.3$  pixels. The symmetry is high along the X-axis, as expected as this is tangential to the off-axis position. There is a linear dependence on field position in Y, which in the table above appears to be decreasing with telescope focus position. This suggests that the sequence has not passed through the best focus position at the end.

One AG focus unit corresponds to a change in telescope focus of  $5.2\mu\text{m}$ , or a M2 movement of  $0.189\mu\text{m}$ . From the first sequence, it is concluded that the AG camera is approximately 200 units out of focus, which corresponds to a M2 movement of  $0.038\text{mm}$ . This is greater than the focus range tested in the second sequence and supports that the small telescope focus change could not fully compensate for the AG camera defocus.

The field dependence of FWHM close to focus is described in the figures below. Further away from focus, the field dependence becomes more pronounced

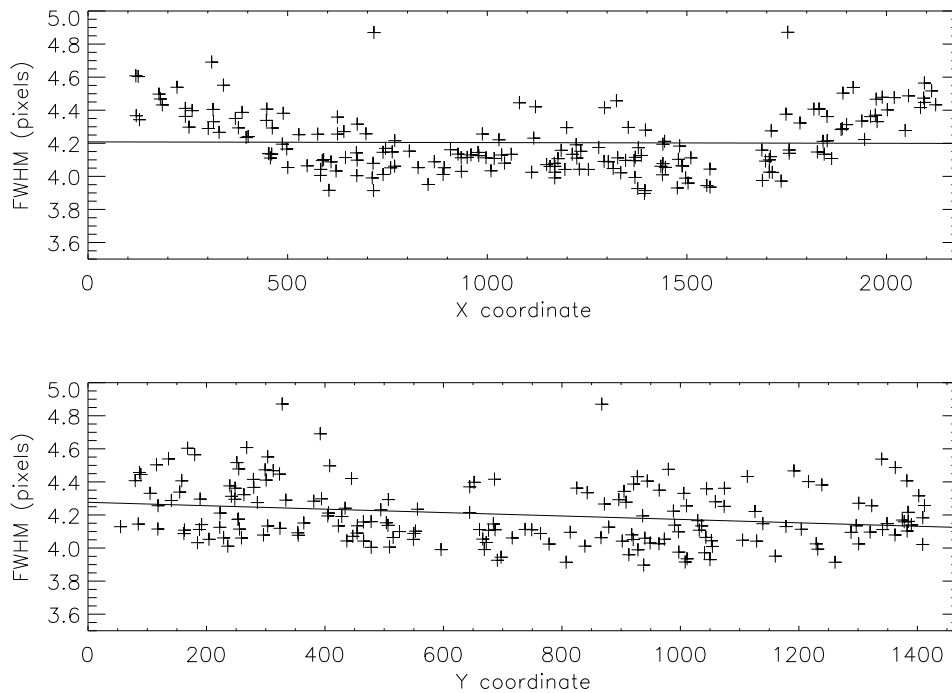


**Figure 2** FWHM distribution along the X and Y axes for telescope focus -1.170mm and AG focus 2000. The distribution in X is symmetric, while a weak gradient in Y is present.

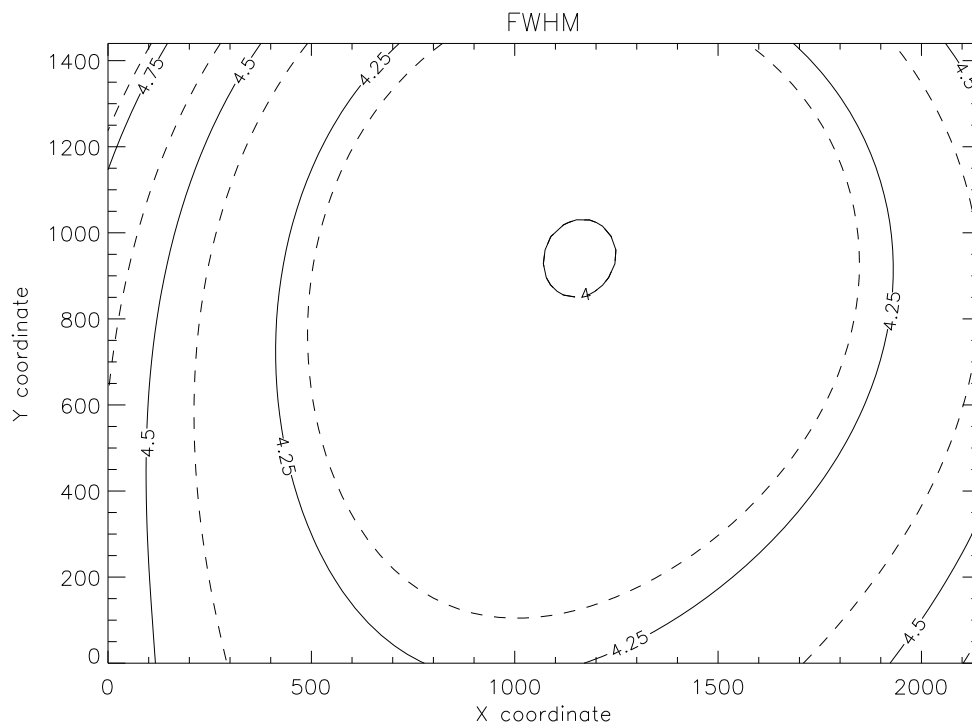


**Figure 3** FWHM distribution over the AG field for telescope focus -1.170mm and AG focus 2000.

## Focus pyramid

The final through-focus sequence mentioned above was repeated with the focus pyramid in the beam. The purpose was to map gain and zero-point values, as well as possible field dependency – a values that are needed to be known before the pyramid can be used for focusing.

The result of identifying and measuring quadrant geometry in the images is summarised in the table below:

Tel-Focus (mm)	Mean diagonal (pixels)	Focus offset (mm)	# quad stars	X-gradient (degrees)	Y-gradient (degrees)
-1.130	27.35 ± 0.05	-0.19	162	-0.23	0.66
-1.150	29.07 ± 0.06	0.53	99	-0.06	0.38
-1.170	29.28 ± 0.05	0.61	143	-0.04	0.38

“Tel-focus” is the encoder position for M2. “Mean diagonal” is calculated from measurements on several quadruple star images identified in the frame. “Focus offset” is the expected distance to Cassegrain focus, derived from the measured diagonal. “# quad stars” is the number of useable quadruple images. The “X/Y gradient” is derived from a linear fit to a field-dependent change in the quadrant diagonals, expressed as a tilt respective to the Cassegrain focal plane.

A movement of M2 by 0.02mm is expected to cause a focus change of 0.55mm. The focus pyramid sensitivity has been determined to 2.43pixels/mm [1], so a 1.33 pixel diagonal change should result from the focus steps applied here. The match is seen to be very poor, compared to the uncertainty on the diagonal length.

The focus offset is determined to the expected target value of 27.85 pixels. The target telescope focus should then be -0.136mm, in contradiction to the result from the FWHM analysis in the previous section. The new target diagonal should be determined on the telescope.

The focal plane tilt in the X-direction is found to be small, in agreement with the FWHM analysis, and a significant tilt is present in the Y-direction.

To correct for the approx 0.4 degree Y-gradient, the three fixing points of the autoguider table can be shimmed. With good approximation the line connecting two of the supporting points are parallel to the reflection direction of the pick-up mirror. The distance between the supports is 347mm, which means that one of the supports must be moved by 2.4mm. According to the sign of the tilt, additional shims of 2.4mm must be placed under the outer support to the same side as the pick-up mirror. I.e. the left-hand support when looking at the autoguider from outside. However, the impact of the tilt on image quality is very small, and this correction is not considered important.

## Throughput

The efficiency of the autoguider optics was estimated relatively to that of HFOSC by observing the same field with both instruments. As the AG-filter transmits in the V, R and part of the I-band, the counts from observations in these filters with HFOSC was added and compared for the counts with the autoguider. The counts were further corrected for the relative CCD QE in the relevant bands and the gain difference. The resulting count ratio was 1.0, indicating equal performance of the two sets of optics. The scatter in ratio was about 15% when using different stars. This is interpreted as a result of colour differences, as the V, R and I filters do not perfectly overlap the AG filter.

Applied correction factors:

Detector	V QE	R QE	I QE	Gain
HFOSC/SITE	65%	65%	53%	1.22
A-G/KAF	50%	62%	30%	1.0

As mentioned in the next section, 1.8KADU/sec was registered from a  $m_v=17$  guide star. This is in good agreement with the expected flux used for the limiting brightness calculations in [1].

## Guiding performance

Installation of the autoguider required an upgrade of the Telescope Control System, which resulted in occasional poor blind tracking. Autoguiding in such conditions resulted in dramatic improvement, as demonstrated in the figure below.

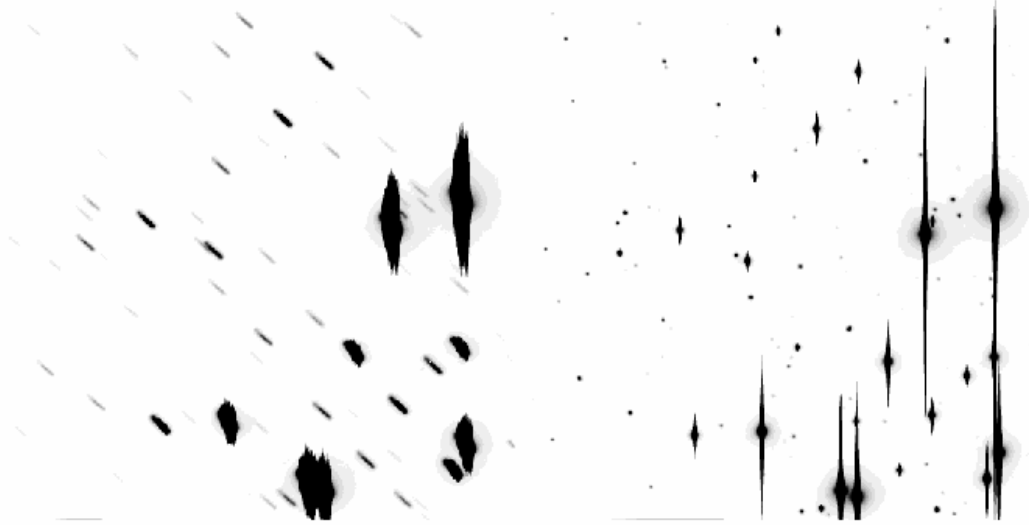


**Figure 4** HFOSC exposures of 600 seconds. Left: blind tracking and right: autoguiding.

At a time where no problems with the new TCS were experienced, a more realistic test was made. A series of 60 second exposures were made with HFOSC while using different modes of guiding. This included using guide exposure and correction cycles of 1 and 4 seconds, guide stars of different brightness and a blind tracking exposure as reference. The blind tracking FWHM is similar to the FWHM registered during guiding, confirming that the TCS behaves well.

Star / exposure ID	Guide star brightness				AG exposure time	HFOSC FWHM (pixels)
	$m_v$	$m_r$	$m_i$	AG counts/sec (ADU)		
/ 15	$\approx 10$	N/A	9	650K	1 sec	4.4
PG2213-006B / 16	12.7	12.3	11.9	85K	-	-
PG2213-006C / 13	15.1	14.7	14.3	8K	1 sec	5.3
/ 10	16.5	15.9	15.4	2.5K	1 sec	8.5
/ 11	16.5	15.9	15.4	2.5K	4 sec	5.0
/ 14	17.1	16.6	16.2	1.8K	4 sec	4.6
Blind tracking	-	-	-	-	-	4.8

The table is sorted by guide star brightness. The faintest star that we successfully guided on was at  $m_v=17$ , using an integration time of 4 seconds. Using an integration time of 1 second on this star was not possible.

The test data is too limited to draw firm conclusions from, but there are some indications:

In two occasions, the FWHM of the guided image was marginally better than of the blind tracking reference. This was while using a fast (1 sec) guide loop on a bright ( $m_v \approx 9$ ) guide star, and while using a slower (4 sec) loop on a faint ( $m_v=17$ ) guide star.

On one occasion, the guided FWHM became much worse than while blind tracking (8.5 vs. 4.8), while using a relatively faint guide star ( $m_v=16.5$ ). The counts per integration were apparently too low. This improved when the exposure time was increased from 1 second to 4 seconds.

According to [1], figure 1, with a full moon sky brightness and a seeing of  $1''3$ , the faintest useable guide star for a 1 second exposure is  $m_v=17.5$ . We have not reached that goal, as a 1 sec guide loop on a  $m_v=16.5$  star did not perform well, and a 4 sec exposure was required on a  $m_v=17.0$  guide star.

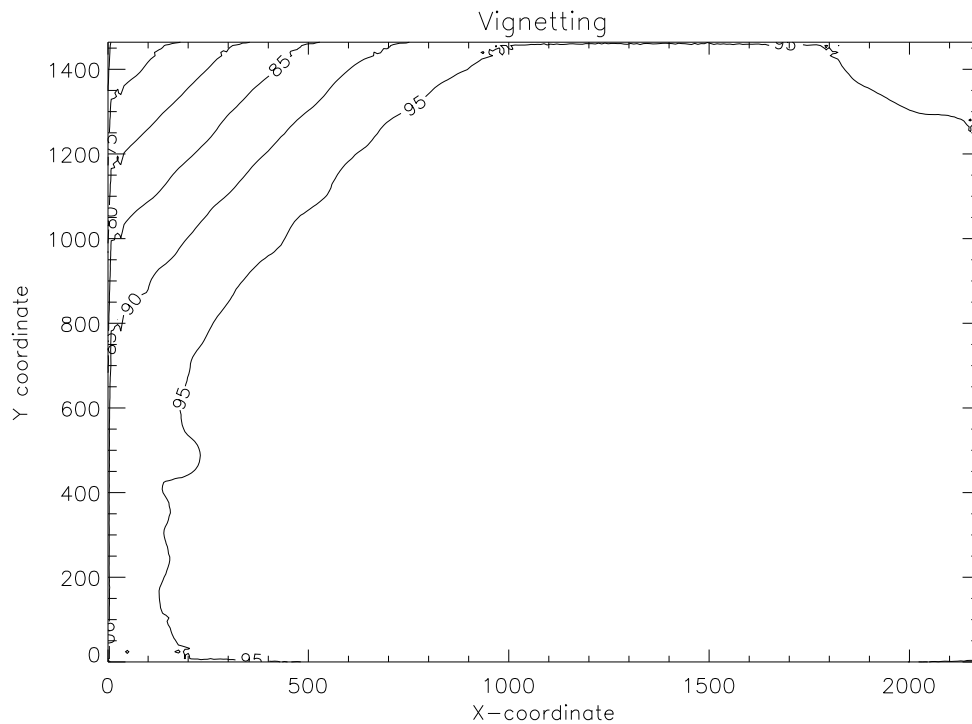
Among the reasons for the requirement for brighter guide stars can be mentioned:

- The prediction was based on the required signal/noise ratio for a quadrant sensor, while a centroid algorithm was used. The centroid is inherently more noise-sensitive.
- At the time of the test, the guide routine had not been optimised to the final level. A too large area of the background was used for centroid determination, while later this was reduced to a smaller field scaled by the FWHM of the guide star profile, giving better S/N.
- The discontinuities in the analog-to-digital conversion, as seen in [1], figure 12, will lead to a higher effective read-out noise.

From this it is estimated that the limiting magnitude is 1.5 brighter than expected, or a factor of 4 in flux. With an exposure time of four seconds, full sky coverage should be ensured.

## Vignetting

The large off-axis field of view was not possible to achieve without accepting some amount of vignetting from the adapter, as described in [1]. This was mapped by examining the moon-light distribution of a frame obtained in complete cloud cover. This is shown in Figure 5. A 20% vignetting was predicted for both of the far corners. This has been offset, so one corner has a maximum vignetting of about 30% and the opposite by less than 10%.



## ***References***

- [1] Optical design of an autoguider for the Hanle Observatory, CUO, August 2005